

Multiscale and Domain Decomposition Methods for Linear and Nonlinear Fracture Network Flows

Konstantin Brenner^[0000-0002-9372-0431],
Géraldine Pichot^[0009-0008-2044-9346],
Daniel Zegarra Vasquez^[0009-0001-5633-2683]

1 Introduction

Fractures play a major role in the transport of mass and energy within subsoil and therefore constitute key objects of interest for numerous industrial processes related to resource extraction and storage. Regarding the modeling of fractured media, several approaches can be distinguished depending on how the geometry of the fracture networks is represented and how interactions with the surrounding medium are taken into account. We refer to [2] for a review on this matter. In this contribution, we focus on so-called Discrete Fracture Network (DFN) models in which fractures are explicitly represented as two-dimensional surfaces, while the surrounding bulk medium is assumed to be impervious. Specifically, we are concerned with incompressible fluid flow in the fracture network, which is assumed to follow mass conservation and two-dimensional Darcy or Darcy–Forchheimer laws [1, 6].

Numerical modeling of flow in fractured media is a challenging task for several reasons. To begin with, information about the actual geometry of the medium is often scarce and must be extrapolated from limited data such as borehole samples and outcrops, leading to a stochastic modeling approach, which in turn raises the problem of generating good-quality computational meshes. Finally, realistic fracture networks typically contain a significant number of fractures, leading to large linear systems that arise from the discretization of the flow equations. In this work, we rely on the approach of [5, 8] for the generation of DFN geometries and meshes, while large algebraic systems resulting from the discretization of linear and nonlinear DFN flow models are handled by means of an MsFEM-like discretization method [7],

Konstantin Brenner
Université Côte d’Azur, Inria, CNRS, LJAD, France, e-mail: konstantin.brenner@univ-cotedazur.fr

Géraldine Pichot · Daniel Zegarra Vasquez
Inria, CERMICS, École Nationale des Ponts et Chaussées, France, e-mail:
geraldine.pichot@inria.fr, daniel.zegarra-vasquez@inria.fr

proposed in [3]. The multi-scale approach, called the Trefftz method, allows us to significantly reduce the size of the problem while keeping reasonable accuracy. We further highlight the possibility of using the obtained coarse approximation method within a two-level Domain Decomposition based on Restricted Additive Schwarz method, leading to an efficient iterative solver that can be used for both linear and nonlinear models. The performance of the Trefftz method is demonstrated using a DFN containing over a thousand fractures.

1.1 Geometry and Darcy flow model

Let $(\Omega_i)_{i \in I}$ denote a finite family of open, simply connected polygons in \mathbb{R}^3 representing fractures, and let $\bar{\Omega} = \bigcup_{i \in I} \bar{\Omega}_i$. For $i, j \in I$ with $i \neq j$, we denote $\Gamma_{ij} = \bar{\Omega}_i \cap \bar{\Omega}_j$ and $\Gamma_{int} = \bigcup_{\substack{i, j \in I \\ i \neq j}} \Gamma_{ij}$. We assume that the set $\bigcup_{i \in I} \partial\Omega_i \setminus \Gamma_{int}$ is partitioned into two non-overlapping domains, Γ_D and Γ_N , where, respectively, Dirichlet and Neumann boundary conditions will be imposed. Figure 1 illustrates a typical partitioning of the domain boundary, where Γ_D corresponds to the intersection of the fracture network with its axis-aligned bounding box, while the remaining portion of the boundary is subject to homogeneous Neumann boundary conditions. The set $\Gamma = \Gamma_{int} \cup \bar{\Gamma}_D$ will be referred to as the *skeleton* of the network.

Let \mathcal{E} denote a partition of Γ into linear elements such that each *coarse edge* $e \in \mathcal{E}$ is a closed segment, and any two distinct elements of \mathcal{E} intersect, if at all, only at their boundaries. We then introduce the set of *nodes* defined by $\mathcal{S} = \bigcup_{e \in \mathcal{E}} \partial e$. Both sets \mathcal{S} and \mathcal{E} are illustrated in Figure 1.

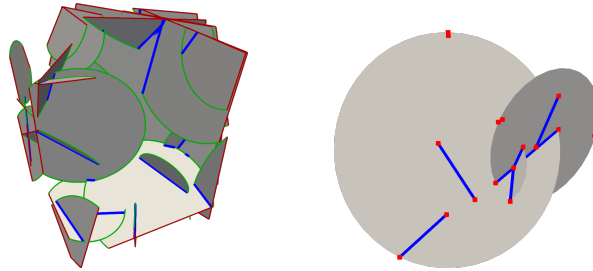


Fig. 1 **Left:** Example of a discrete fracture network (DFN) with a partitioned boundary. The interior skeleton Γ_{int} is shown in blue, the Dirichlet Γ_D and Neumann Γ_N boundaries are highlighted in red and green, respectively. **Right:** Illustration of the set of nodes \mathcal{S} (shown as red dots) and the coarse edges \mathcal{E} (shown in blue).

In order to give the weak formulation of the linear Darcy flow model, we introduce the following Hilbert spaces

$$H^1(\Omega) = \{v = (v_i)_{i \in I} \mid v_i \in H^1(\Omega_i) \text{ and } v_i|_{\Gamma_{ij}} = v_j|_{\Gamma_{ij}} \text{ for all } i \neq j, i, j \in I\}$$

and

$$H_{\Gamma_D}^1(\Omega) = \{v \in H^1(\Omega) \mid v_i|_{\partial\Omega_i \cap \Gamma_D} = 0 \text{ for all } i \in I\}.$$

Let us denote

$$a(u, v) = \sum_{i \in I} \int_{\Omega_i} \nabla_i u_i \cdot \nabla_i v_i \, d\omega(\mathbf{x}) \quad \text{and} \quad l(v) = \sum_{i \in I} \int_{\Omega_i} f v_i \, d\omega(\mathbf{x}),$$

where ∇_i stands for the tangential gradient operator, defined by fixing a reference Cartesian coordinate system in the plane containing the fracture Ω_i . The weak formulation of the Darcy flow model [1] reads as: Find $u \in H_{\Gamma_D}^1(\Omega)$ such that

$$a(u, v) = l(v) \quad \forall v \in H_{\Gamma_D}^1(\Omega). \quad (1)$$

Assuming that Ω is connected and that Γ_D is non-empty, it is easy to show the wellposedness of the latter problem.

The linear variational equality (1) serves as our primary model problem, along with its nonlinear extension given by the Darcy–Forchheimer model [6], which is going to be introduced in Section 2.

2 Trefftz method for linear and nonlinear DFN flow models

The Trefftz method is built upon an orthogonal decomposition of $H^1(\Omega)$ into the direct sum of the space of “bubbles”

$$H_{\Gamma}^1(\Omega) = \{v \in H^1(\Omega) \mid v|_{\Gamma} = 0\},$$

and the space of locally harmonic functions

$$H_{\Delta}^1(\Omega) = \{v \in H^1(\Omega) \mid a(v, w) = 0 \quad \text{for all } w \in H_{\Gamma}^1(\Omega)\}.$$

These two spaces are orthogonal with respect to the bilinear form a , so that the original problem is equivalent to: Find $u = u_{\Delta} + u_{\Gamma}$ with $u_{\Delta} \in H_{\Delta}^1(\Omega) \cap H_{\Gamma_D}^1(\Omega)$ and $u_{\Gamma} \in H_{\Gamma}^1(\Omega)$ such that

$$\begin{cases} a(u_{\Delta}, v) = l(v) \text{ for all } v \in H_{\Delta}^1(\Omega) \cap H_{\Gamma_D}^1(\Omega), \\ a(u_{\Gamma}, v) = l(v) \text{ for all } v \in H_{\Gamma}^1(\Omega). \end{cases}$$

Because the bubble component u_{Γ} can be (approximately) determined independently for every Ω_i , we will focus on the approximation of the globally coupled, locally harmonic component u_{Δ} . The former is achieved by elliptic projection of u_{Δ} on a finite-dimensional subspace of $H_{\Delta}^1(\Omega)$. We first introduce the space

$$V_{H,r}^{\Gamma} = \{v \in C^0(\Gamma) \mid v|_e \in \mathbb{P}_r(e) \quad \text{for all } e \in \mathcal{E}\},$$

where $\mathbb{P}_r(e)$ denotes the set of polynomials defined over an edge e of order (at most) r , while $C^0(\Gamma)$ is understood as a set of functions continuous over each connected component of Γ . The Trefftz method is based on the space

$$V_{H,r} = \{v \in H_\Delta^1(\Omega) \mid v|_\Gamma \in V_{H,r}^\Gamma\}.$$

Using the space $V_{H,r}$, the locally harmonic component of the solution u_Δ can be approximated by $u_H \in V_{H,r} \cap H_{\Gamma_D}^1(\Omega)$ such that

$$a(u_H, v) = l(v) \quad \text{for all } v \in V_{H,r} \cap H_{\Gamma_D}^1(\Omega). \quad (2)$$

Now, let us consider the Darcy-Forchheimer model [6], for which we seek an approximate solution $u_H \in V_{H,r} \cap H_{\Gamma_D}^1(\Omega)$ such that, for any $v \in V_{H,r} \cap H_{\Gamma_D}^1(\Omega)$, it holds

$$\sum_{i \in I} \int_{\Omega_i} \psi(|\nabla_i(u_H)_i|) \nabla_i(u_H)_i \cdot \nabla_i v_i \, d\omega(\mathbf{x}) = \sum_{i \in I} \int_{\Omega_i} f v_i \, d\omega(\mathbf{x}). \quad (3)$$

with $\psi(a) = \frac{\sqrt{1 + 4\beta a} - 1}{2\beta a}$. We note that the linear Darcy model is recovered at the limit when β goes to zero.

2.1 Fine-scale problem, approximation of $V_{H,r}^\Gamma$ and two-level solvers

Let $(\phi_{\Gamma,l})_{l=1,\dots,N_H}$ denote the nodal Lagrange basis of $V_{H,r}^\Gamma$, and we will denote by $(\phi_l)_{l=1,\dots,N_H}$ the basis in $V_{H,r}$ obtained by the harmonic extension of $\phi_{\Gamma,l}$ over Ω . Because, in general, the basis of $V_{H,r}$ cannot be expressed analytically, we proceed with its approximation using a *fine-scale* discretization method.

Let us consider a triangulation of Ω which is assumed to be conforming with respect to the partitioning $(\Omega_i)_{i \in I}$. We then use this triangulation to discretize (1) based on a continuous Lagrange finite element method, which leads to the following *fine-scale* linear system

$$A\mathbf{u} = \mathbf{f}, \quad (4)$$

where A is an $N \times N$ finite element stiffness matrix.

Let R_Γ and $R_{\Omega \setminus \Gamma}$ denote the Boolean restriction matrices associated with the subsets of the fine-scale degrees of freedom located on the skeleton Γ and $\Omega \setminus \Gamma$ respectively, with respective sizes $N_\Gamma \times N$ and $N_{\Omega \setminus \Gamma} \times N$. Note that $N_\Gamma + N_{\Omega \setminus \Gamma} = N$. We denote by ϕ_l the approximation of ϕ_l and we set $\phi_l = R_{\Omega \setminus \Gamma}^T \phi_{\Omega \setminus \Gamma, l} + R_\Gamma^T \phi_{\Gamma, l}$, where $\phi_{\Gamma, l}$ is defined by evaluating ϕ_l at the fine-scale degrees of freedom located on Γ , while the extension $\phi_{\Omega \setminus \Gamma, l}$ is defined by solving $(R_{\Omega \setminus \Gamma} A R_{\Omega \setminus \Gamma}^T) \phi_{\Omega \setminus \Gamma, l} = -(R_{\Omega \setminus \Gamma} A R_\Gamma^T) \phi_{\Gamma, l}$. We note that for every coarse dof l the latter system can be

localized to a handful of subdomains sharing this dof. We remark that the dofs of the lowest-order coarse space $V_{H,1}$ are associated with the coarse nodes of \mathcal{S} .

We further introduce the $N_H \times N$ transition matrix \mathbf{R}_H , such that the l th row of R_H is given by ϕ_l^T . With that, the discrete counterpart of (2) writes as

$$A_H \mathbf{u}_H = \mathbf{f}_H, \quad \text{with} \quad A_H = R_H A R_H^T \quad \text{and} \quad \mathbf{f}_H = R_H \mathbf{f}. \quad (5)$$

Similarly, for the nonlinear model, let $F : \mathbb{R}^N \rightarrow \mathbb{R}^N$ denote the residual function resulting from the fine-scale approximation of (3). Its coarse approximation writes as the following system

$$R_H F(R_H^T \mathbf{u}_H) = 0. \quad (6)$$

We note that, provided that the initial guess \mathbf{u}_0 belongs to $\text{Im}(R_H^T)$, Newton's method applied to (6) can be expressed as

$$\mathbf{u}_{n+1} = \mathbf{u}_n - R_H^T J_H(\mathbf{u}_n)^{-1} R_H F(\mathbf{u}_n), \quad J_H(\mathbf{u}) = R_H F'(\mathbf{u}) R_H^T, \quad (7)$$

where F' denotes the Gâteaux derivative of F .

Let $(\Omega'_i)_{i \in I}$ denote the overlapping partitioning of Ω such that $\Omega_i \subset \Omega'_i$. In practice, we construct the sub-domain Ω'_i by propagating Ω_i by one layer of triangles. Let N_i be the number of degrees of freedom contained in $\overline{\Omega'_i}$. We denote by R_i the $N_i \times N$ Boolean restriction matrix associated with the subsets of fine-scale degrees of freedom belonging to $\overline{\Omega'_i}$. Further, let D denote the partition of unity matrix associated with this decomposition of the degrees of freedom, defined as $D = (\sum_{i \in I} R_i^T R_i)^{-1}$, and let $D_i = R_i D R_i^T$. Let $F : \mathbb{R}^N \rightarrow \mathbb{R}^N$ denote the residual function of the systems resulting from the fine-scale finite element discretization of either the Darcy or Darcy-Forchheimer model, and let \mathbf{u}_0 be the initial guess given, for example, by $\mathbf{u}_0 = R_H^T \mathbf{u}_H$ with \mathbf{u}_H satisfying either (5) or (6). We define the following two-level iterative algorithm based on the Restricted Additive Schwarz (RAS) method that multiplicatively combines a sub-domain correction

$$\mathbf{u}_{n+\frac{1}{2}} = \mathbf{u}_n - \sum_{i \in I} R_i^T D_i J_i(\mathbf{u}_n)^{-1} R_i F(\mathbf{u}_n), \quad J_i(\mathbf{u}) = R_i F'(\mathbf{u}) R_i^T, \quad (8)$$

with a coarse correction

$$\mathbf{u}_{n+1} = \mathbf{u}_{n+\frac{1}{2}} - R_H^T J_H(\mathbf{u}_{n+\frac{1}{2}})^{-1} R_H F(\mathbf{u}_{n+\frac{1}{2}}), \quad J_H(\mathbf{u}) = R_H F'(\mathbf{u}) R_H^T. \quad (9)$$

We note that the coarse correction step (9) coincides with (7).

3 Numerical experiment

We consider a large network shown in Figure 2. The network accounts for approximately 1.4 k fractures contained in an axis-aligned cube $Q = [-L, L]^3$, $L = 10 m$.

The skeleton Γ of the network accounts for roughly $5.4k$ edges and about $7.2k$ coarse nodes. The fine-scale triangulation has about $178k$ triangles and $96k$ points. Because the network contains a few large fractures, we constrain the maximum length of the coarse edges to be below $2m$.

We examine both linear Darcy and nonlinear Darcy-Forchheimer flow problems with zero right-hand side. For the boundary conditions we consider three flow scenarios in which Dirichlet boundary conditions are imposed on two opposite sides of $Q \cap \bar{\Omega}$, while the remainder of the boundary is subject to zero Neumann conditions. Specifically, for $\alpha = 1, 2, 3$, we define $\Gamma_{D,-L} = \bar{\Omega} \cap \{(x_1, x_2, x_3) \mid x_\alpha = -L\}$ and $\Gamma_{D,L} = \bar{\Omega} \cap \{(x_1, x_2, x_3) \mid x_\alpha = L\}$, and we set $u|_{\Gamma_{D,-L}} = 1$ and $u|_{\Gamma_{D,L}} = 0$. We consider the parameter β of the Darcy-Forchheimer model taking values 4 or 8. For the fine-scale approximation, we employ continuous piecewise affine finite elements, and the polynomial degree r of the Trefftz method is also set to one.

For each of the flow scenarios we evaluate the accuracy of the Trefftz method and report the associated computation time in comparison to the fine-scale finite element calculation. The results are summarized in Table 1. Both coarse and fine-scale linear systems are solved using Cholesky factorization [4] from *SuiteSparse* library. We acknowledge the fact that a fair evaluation of the Trefftz method should include the time required for the computation of the Trefftz method's basis functions as well as the assembly of the coarse system. Due to their local nature, those calculations can and should be performed in parallel, which is typical for multi-scale methods. However, the evaluation of the parallel performance of the method is not included in this article and will be communicated in the future.

Main flow direction	Darcy			DF $\beta = 4$			DF $\beta = 8$		
	$\alpha = 1$	$\alpha = 2$	$\alpha = 3$	$\alpha = 1$	$\alpha = 2$	$\alpha = 3$	$\alpha = 1$	$\alpha = 2$	$\alpha = 3$
Rel. L^2 error	0.2%	0.1%	0.1%	0.5%	0.4%	0.4%	0.6%	0.5%	0.5%
Rel. H^1 error	8.9%	7.6%	7.5%	17.4%	13.2%	13.3%	20.0%	14.9%	15.1%
Rel. flux error	0.8%	0.6%	0.6%	1.9%	1.4%	1.4%	2.3%	1.6%	1.6%
Fine sol. time (s)	0.16	0.17	0.19	1.0	1.1	1.1	0.9	1.2	1.3
Coarse sol. time (s)	0.026	0.037	0.034	0.15	0.15	0.15	0.16	0.17	0.21
Speedup	6.0	4.6	5.7	6.9	7.2	7.8	5.5	7.1	6.1

Table 1 Relative errors, solution times, and the speedup per main flow direction for Darcy and Darcy-Forchheimer models.

We report in Table 1 the relative difference between the approximate solution obtained by the Trefftz and the fine-scale finite element methods. The error is reported in the L^2 norm and the H^1 semi-norm. Additionally, we communicate the accuracy of the approximation of the total outflow through the boundary $\Gamma_{D,L}$. For the linear model, the outflow error is computed as

$$err_{flux} = \frac{\mathbf{i}_{\Gamma_{D,L}} A_{\text{Neumann}} (\mathbf{u} - R_H^T \mathbf{u}_H)}{\mathbf{i}_{\Gamma_{D,L}} A_{\text{Neumann}} \mathbf{u}},$$

where \mathbf{u} and \mathbf{u}_H solve (4) and (5) respectively, A_{Neumann} is the system matrix resulting from the fine-scale discretization of the Neumann problem, and $\mathbf{i}_{\Gamma_{D,L}}$ is an “indicator vector of $\Gamma_{D,L}$ ”, that is

$$(\mathbf{i}_{\Gamma_{D,L}})_j = \begin{cases} 1 & \text{if } x_j \in \Gamma_{D,L}, \\ 0 & \text{else.} \end{cases}$$

We proceed similarly for the Darcy-Forchheimer model.

The performance of the Trefftz method is fairly consistent across both linear and nonlinear flow simulations, as well as for all three flow scenarios. The error is systematically larger in the nonlinear case and tends to increase with higher values of the parameter β . The L^2 error is low and remains between 0.1% and 0.6% regardless of the flow direction or the model used. The error measured in the H^1 semi-norm is higher, ranging from 7% to 9% for the linear model and from 13% to 17% for the nonlinear one. Despite the higher H^1 error, the approximation of the total outflow remains reasonably accurate, with errors below 2.5% in all cases. The coarse system is approximately 13.5 times smaller than the one obtained from the fine-scale discretization, and a computational speedup between 4.5 and 8 is observed. The fact that the speedup does not fully match the system size ratio can be attributed to the higher density of the coarse system matrix, which, on average, has about 48 non-zero elements per row.

Next, for both linear and nonlinear flow models, we evaluate the performance of the two-level iterative method (8)–(9) referred to as RAS2. Figure 2 shows the convergence of the relative error measured in the H^1 semi-norm. The initial points correspond to the Trefftz method approximation. The convergence of the method (8)–(9) is depicted by the blue, green, and violet curves for, respectively, the linear and two nonlinear models with $\beta = 4$ and $\beta = 8$. We observe a fast initial decay of the error, followed by slower convergence in the linear and nonlinear $\beta = 4$ case, or divergence in the case $\beta = 8$. Furthermore, we combine the iterative scheme (8)–(9) with GMRes and Anderson acceleration methods for the linear and nonlinear models, respectively. The use of acceleration techniques results in rapid convergence, which appears to be largely insensitive to the value of the parameter β .

4 Conclusion

We introduced a Trefftz-based multiscale method for incompressible flow in discrete fracture networks governed either by the Darcy, or the Darcy–Forchheimer law. The method relies on a reduced space built by harmonic extensions of polynomial traces defined over the network’s skeleton. Numerical tests on a large DFN show that the method maintains low L^2 errors and accurate total flux representation, while reducing the system size by over an order of magnitude, and, thus, achieving notable computational speedups. The resulting coarse space also functions effectively within a two-level overlapping Schwarz framework.

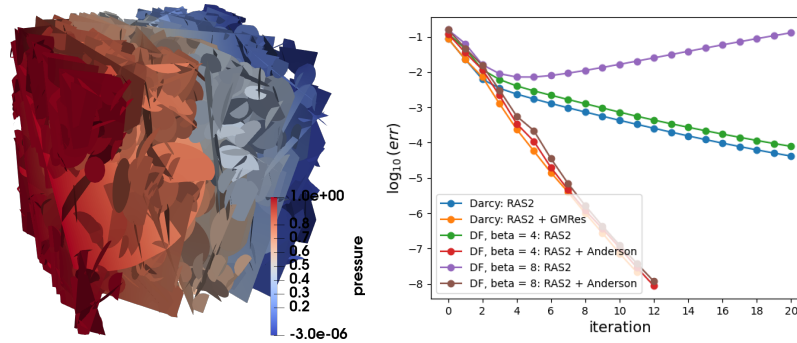


Fig. 2 **Left:** Fracture network and the approximate solution of the Darcy flow problem with unit pressure drop imposed in the x_1 direction. **Right:** Convergence of RAS2 method for Darcy and Darcy-Forchheimer models, with and without acceleration.

Acknowledgements This work has been supported by ANR Project Top-up (ANR-20-CE46-0005).

References

1. Alboin, C., Jaffré, J., Roberts, J.E., Serres, C., et al.: Modeling fractures as interfaces for flow and transport in porous media. *Contemp. Math.* **295**, 13–24 (2002)
2. Berre, I., Doster, F., Keilegavlen, E.: Flow in fractured porous media: a review of conceptual models and discretization approaches. *Transp. Porous Media* **130**(1), 215–236 (2019)
3. Boutilier, M., Brenner, K., Dolean, V.: Robust methods for multiscale coarse approximations of diffusion models in perforated domains. *Appl. Numer. Math.* **201**, 561–578 (2024)
4. Chen, Y., Davis, T.A., Hager, W.W., Rajamanickam, S.: Algorithm 887: CHOLMOD, supernodal sparse Cholesky factorization and update/downdate. *ACM Trans. Math. Softw.* **35**(3), 1–14 (2008)
5. Davy, P., Le Goc, R., Darcel, C., Bour, O., de Dreuzy, J.R., Munier, R.: A likely universal model of fracture scaling and its consequence for crustal hydromechanics. *J. Geophys. Res. Solid Earth* **115**(B10) (2010)
6. Frih, N., Roberts, J.E., Saada, A.: Modeling fractures as interfaces: a model for Forchheimer fractures. *Comput. Geosci.* **12**(1), 91–104 (2008)
7. Hou, T.Y., Wu, X.H.: A multiscale finite element method for elliptic problems in composite materials and porous media. *J. Comput. Phys.* **134**(1), 169–189 (1997)
8. Laug, P., Pichot, G.: Mesh generation and flow simulation in large tridimensional fracture networks. In: S. Carillo, C. Conti, D. Mansutti, F. Pitolli, R.M. Spitaleri (eds.) *IMACS Ser. Comput. Appl. Math.*, vol. 22, pp. 71–80 (2019)